Thermodynamics of Metal Reactants for Ammonia Synthesis from Steam, Nitrogen and Biomass at Atmospheric Pressure

Ronald Michalsky and Peter H. Pfromm
Dept. of Chemical Engineering, Kansas State University, Manhattan, KS 66506

DOI 10.1002/aic.13717
Published online December 29, 2011 in Wiley Online Library (wileyonlinelibrary.com).

Catalytic ammonia synthesis at approximately 30 MPa and 800 K consumes about 5% of the global annual natural gas production causing significant CO_2 emissions. A conceptual solar thermochemical reaction cycle to produce NH_3 at near atmospheric pressure without natural gas is explored here and compared to solar thermochemical steam/air reforming to provide H_2 used in the Haber-Bosch process for NH_3 synthesis. Mapping of Gibbs free energy planes quantifies the tradeoff between the yield of N_2 reduction via metal nitridation, and NH_3 liberation via steam hydrolysis vs. the temperatures required for reactant recovery from undesirably stable metal oxides. Equilibrium composition simulations suggest that reactants combining an ionic nitride-forming element (e.g., Mg or Ce) with a transition metal (e.g., $MgCr_2O_4$, $MgFe_2O_4$, or $MgMoO_4$) may enable the concept near 0.1 MPa (at maximum 64 mol % yield of Mg_3N_2 through nitridation of $MgFe_2O_4$ at 1,300 K, and 72 mol % of the nitrogen in Mg_3N_2 as NH_3 during hydrolysis at 500 K). *AIChE J,* 58: 3203–3213, 2012
Keywords: ammonia, fertilizer, solar energy, thermochemical reaction cycle, low pressure, fossil fuel

Introduction

Agriculture is faced with an increasing demand for production due to a growing and developing world population.[1] The global average nitrogen demand for fertilization is about 2.6 to 2.9 kg nitrogen/year/capita, and this demand is satisfied mainly by ammonia and ammonia-derived materials such as urea.[1]

The expanded renewable fuel standard (RFS2) requires that in the U.S. the annual use of 3.4×10^7 m^3 of biofuel (e.g., from corn or cellulosic biomass) in 2008 is to be increased to about 1.4×10^8 m^3 in 2022.[2]

Ammonia-based fertilizers play a crucial role to satisfy both the demands for food and biofuels. The chemical industry supplies the majority of fertilizers (mainly liquid NH_3, $(NH_2)_2CO$, NH_4NO_3, $(NH_4)_2SO_4$, K_2O, P_2O_5, and various mixtures of these materials) to agriculture. The Haber Bosch process introduced at industrial scale in 1913[1] synthesizes the vast majority of the 1.28×10^8 metric tons of the NH_3 produced globally (2001)[3] via catalytic synthesis of NH_3 from a stoichiometric mixture of N_2 and H_2 at 30 MPa and 700–900 K. This requires technologically sophisticated high pressure and high-temperature operations that are capital intensive and dictate the need for large facilities producing at above 1,000 t NH_3/day. The process reaches ideally 22.7 mol % conversion of $^1/_2$ N_2 to NH_3 (estimated via Gibbs free energy minimization, Aspen Plus V7.2). The overall process including H_2 production generates about 2.3 t of fossil-derived CO_2 per t of NH_3,[4] and expends 2% of the world's energy budget[5] in the form of natural gas (about 28–37 GJ/t NH_3 in North America[4,6]). Steam-reforming of coal instead of using natural gas (a frequent practice in India and China) requires even more energy (about 48–166 GJ/t NH_3[4,7]). This causes generation of 16.7 t CO_2 per t NH_3 produced.[4] Production costs of NH_3 (and, thereby, to some extent food or biofuel prices) are tied closely to the volatility of natural gas prices, and also to existing or anticipated CO_2 emission regulations.

Nitrogen fixation remains a challenge. The dependence on natural gas, the technically demanding process conditions, the CO_2 emissions, and the economy of scale all motivate continued interest in NH_3 synthesis. Potential use of NH_3 as a H_2 carrier molecule,[8,9] or as a way to store intermittent solar energy[10–12] could also be cited as motivation.

Alternatives to the current industrial NH_3 synthesis

Investigated as alternatives to the Haber-Bosch process, NH_3 synthesis at mild conditions in the liquid phase via transition metal coordination complexes[13] or electrochemical NH_3 synthesis[14,15] have not yet reached maturity. Only modest conversions caused by a low conductivity in the working electrode,[15] and significant amounts of electrical energy required are concerns for electrochemical NH_3 synthesis. NH_3 production from electrolysis of H_2O as attempted in the 1920s has been reported to consume about 90 GJ/t NH_3.[16] This approach would cause a substantial consumption of fossil fuels with the current energy mix to generate electricity (e.g., 49 or 81% of the total electricity in the U.S. or China, respectively, is generated via combustion of coal[17]). Solar energy for splitting H_2O to generate H_2[11,12] for subsequent

Additional Supporting Information may be found in the online version of this article.

R. Michalsky is NSF IGERT associate in biorefining.
Correspondence concerning this article should be addressed to P. H. Pfromm at pfromm@ksu.edu.

NH_3 synthesis via the Haber-Bosch reaction would alleviate the consumption of natural gas for fertilizer production (84% of the energy required for industrial NH_3 synthesis via the Haber-Bosch process is absorbed in steam reforming with natural gas to produce H_2[4]). The Haber-Bosch process itself and the associated challenges would remain. This approach is further discussed later in the section "Process viability".

From the various inorganic routes proposed in the chemical literature for NH_3 synthesis,[18–21] few received greater attention than Frank and Caro who commercialized around 1910 a three-step process producing NH_3 via hydrolysis of calcium cyanamide (a salt-like compound containing reduced nitrogen in form of CN_2^{2-} ions).[16,19,22] To regenerate calcium cyanamide, calcium carbonate (formed during hydrolysis) is heated to form calcium oxide, which is mixed and reacted with coke to yield calcium carbide (about 50 mol % at above 2,100 K[23]). The carbide reacts at decreased temperatures with N_2 recovering calcium cyanamide. Consumption of coke and the technically demanding process temperatures established with an electric furnace translated into an energy consumption of about 210 GJ/t NH_3,[16] which rendered the process economically unattractive.

Thermochemical NH_3 synthesis from a metal nitride/oxide reaction cycle

Based on Serpek's process developed at the beginning of the last century[19–21], reactive NH_3 synthesis was demonstrated successfully via a two-step solar thermochemical cycle of aluminum nitride hydrolysis around 1,300 K and carbothermal reduction and nitridation of aluminum oxide in the range of 2,023–2,273 K.[10,24–26] Similar to the calcium cyanamide cycle, this process forms NH_3 near 0.1 MPa without the need of a fossil H_2 source and in the absence of a catalyst. High-temperatures required for reactant recycling can be provided sustainably by use of abundant solar radiation. Intermittently available solar energy is stored advantageously as NH_3,[11,12] similar to solar thermochemical H_2-production via H_2O-cleavage with a zinc reactant.[11] However, physical containment of these significant reaction temperatures is technically challenging[11,12] and requires sophisticated construction materials and reactor designs.[12,21]

Focusing on the simpler concept of a nitride-based NH_3 synthesis at near ambient pressure and without natural gas, this work pursues a reactant composition which allows the nitride-based NH_3 synthesis at temperatures where relatively common materials of construction (e.g., specialty steels and common ceramics) are stable and available as finished objects and machinable stock. The choice of reducing agent (carbonaceous, hydrogen, or none) affecting process economics is discussed briefly.

The following section assesses the viability of a nitride-based NH_3 synthesis process at an overview level. The section concludes with a list of desirable material properties of the reactant that may allow this concept to be competitive with other NH_3 production schemes. Thereafter, a thermodynamic rationale is proposed to guide the reactant choice. With regard to the quantified tradeoff between high-metal oxide reduction temperatures and high yields of N_2 fixation and NH_3 liberation, a few chemical elements that appear promising for the development of a composite reactant are highlighted. Gibbs free energy computations and simulations of chemical equilibrium compositions focus on magnesium-based reactants to point out possible process limitations and options (e.g., the possibility to decrease the oxide reduction temperature by doping the reactant with transition metals). Both, direct conversion of the metal oxide to a metal nitride (dependent on the thermodynamic stability of the nitride at elevated temperatures) or intermediate formation of a metal vapor is considered. To aid the direct oxide-to-nitride route, cerium is discussed as a candidate to increase the stability of the nitride.

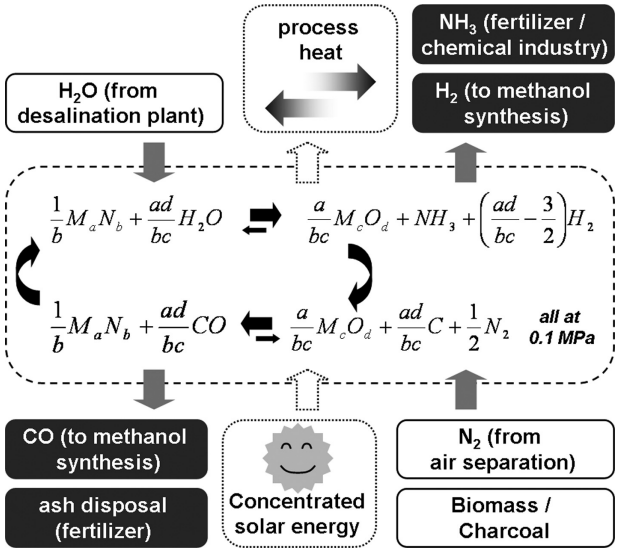

Figure 1. Conceptual approach of Reactive NH_3 Synthesis at atmospheric pressure via a two-step reaction cycle of metal nitride hydrolysis and carbothermal metal oxide nitridation.

Process Concept for Solar Thermochemical NH_3 Synthesis

A solar thermochemical cycle producing NH_3 at atmospheric pressure (Figure 1) by metal nitride hydrolysis and subsequent metal reactant recycling using a carbonaceous reducing agent (e.g., biomass) may be written with generalized stoichiometry as

$$\frac{a}{bc}M_cO_d + \frac{ad}{bc}C \leftrightarrow \frac{a}{b}M + \frac{ad}{bc}CO \quad (1)$$

$$\frac{a}{b}M + \frac{1}{2}N_2 \leftrightarrow \frac{1}{b}M_aN_b \quad (2)$$

$$\frac{1}{b}M_aN_b + \frac{ad}{bc}H_2O \leftrightarrow \frac{a}{bc}M_cO_d + NH_3 + \left(\frac{ad}{bc} - \frac{3}{2}\right)H_2 \quad (3)$$

with M being a metal. Lower case letters indicate stoichiometric coefficients. Carbothermal reduction of M_cO_d (Eq. 1) generates a metal capable of breaking the N_2 triple bond via formation of a metal nitride (M_aN_b) (Eq. 2). The nitride is then corroded during nitride hydrolysis (Eq. 3) forming the metal oxide, the desired NH_3, and possibly H_2. Oxide reduction (Eq. 1) may occur concurrently with metal nitridation (Eq. 2), see section "Step two: Formation of Mg_3N_2".

Process viability

As a first approximation, Figure 2 shows a mass and energy balance-based process analysis for solar thermochemical NH_3 synthesis via an inorganic MgO/Mg_3N_2 cycle (i.e., in Eqs. 1–3, M = Mg, assuming that MgO can be reduced at 1,800 K, see "Promising elements for the nitride formation

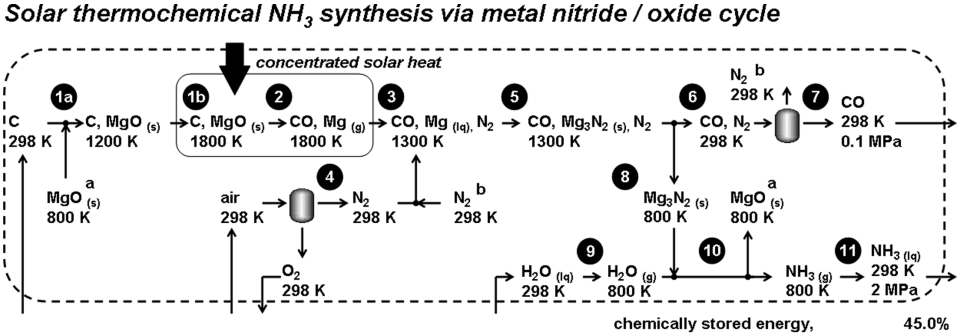

label	process	heat (kJ/mol NH_3)
1a	heat exchange (from process heat)	71.5
1b	heat exchange (from solar heat)	77.1
2	$\Delta_{rxn}H$ for MgO reduction (from solar heat)	917.3
3	heat released to quench gas (N_2)	- 239.2
4	N_2 separation [A]	0.3
5	$\Delta_{rxn}H$ from Mg_3N_2 formation (to steam [B])	- 244.8
6	heat exchange (to steam [B])	- 274.5
7	CO separation [A]	9.7
8	heat exchange (to steam [B])	- 27.8
9	heat exchange (from process heat)	98.2
10	$\Delta_{rxn}H$ from NH_3 formation (to steam [B])	- 352.7
11	heat exchange and compression (net to steam [B])	- 7.1

chemically stored energy, 45.0%
$f_{fuel} = \Delta_{rxn}G_{298K}(NH_3 + 3/4O_2 \rightarrow 1/2N_2 + 3/2H_2O) + \Delta_{rxn}G_{298K}(3/2CO + 3/4O_2 \rightarrow 3/2CO_2) / E_{total,in}$ [C]

energy converted to electricity, 29.2%
f_{elec} = *electricity from steam* [B] / $E_{total,in}$ [C]

total process efficiency, 74.2%
$\eta_{total} = f_{fuel} + f_{elec}$

solar energy integration, 62.7%
f_{solar} = *solar heat*$_{in}$ / $E_{total,in}$ [C]

C-neutral CO generation 1.28 mol/MJ
3/2 mol CO / (η_{total} x $E_{total,in}$ [C])

Figure 2. To assess process viability (compare to Figure 3).

All total pressures are 0.1 MPa except if indicated otherwise; critical separation steps are marked with a gray reactor symbol; energy required for pumping is disregarded. (A) as process steam that is required to generate electricity, and (B) steam used to generate electricity at Carnot efficiency; (C) $E_{total,in}$ = (solar heat at (1b) and (2) + lower heating value of the coal used), absorption losses not accounted.

and NH_3 liberation step''). A similar analysis for solar-driven steam and air reforming to generate H_2 from water and N_2 from air, followed by the conventional Haber-Bosch synthesis is summarized in Figure 3. Major conclusions are:

In the nitride-based process about 74% of the energy input (absorbed solar heat and charcoal) are recovered in form of chemical energy (45% in NH_3, CO) and electricity (29%). The large fraction of produced electricity is due to the heat released from exothermic reactions at decreased temperatures (label 5 and 10, Figure 2) limiting heat integration. Also, the high-reduction temperature of MgO leads to an increased amount of sensible and latent heat in the gaseous products of the oxide reduction step (label 3) which is converted partly to electricity (label 6). The total energy efficiency of the reforming-based process is estimated analogously at 65% (Figure 3). Comparing these figures to the current industrial NH_3 synthesis (ranging from 12% with coal to 69% with natural gas[4]), or the industrial utilization of absorbed solar thermal energy (e.g., about 30% annual average, Andasol power plant, Spain[27]) or coal (35% without CO_2 capture technology[28]) to useful energy in form of electricity, both the solar nitride-based and the solar steam reforming/Haber-

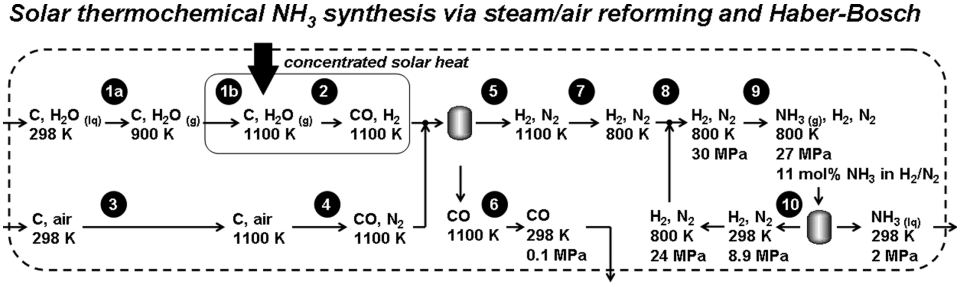

label	process	heat (kJ/mol NH_3)
1a	heat exchange (from process heat)	128.2
1b	heat exchange (from solar heat)	24.8
2	$\Delta_{rxn}H$ for charcoal/steam reforming (from solar heat)	204.9
3	heat exchange (from process heat)	22.6
4	$\Delta_{rxn}H$ from charcoal/air reforming (integrated [A])	- 28.1
5	CO separation [B]	32.5
6	heat exchange (integrated [A])	- 48.1
7	heat exchange (integrated [A])	- 20.4
8	synthesis gas compression [B]	216.8
9	$\Delta_{rxn}H$ from NH_3 formation	- 54.1
10	NH_3 separation loop [B, C]	21.6

total process efficiency, 65.4%
$\eta_{total} = f_{fuel} = \Delta_{rxn}G_{298K}(NH_3 + 3/4O_2 \rightarrow 1/2N_2 + 3/2H_2O) + \Delta_{rxn}G_{298K}(7/4CO + 7/8O_2 \rightarrow 7/4CO_2) / E_{total,in}$

solar energy integration, 19.3%
f_{solar} = *solar heat*$_{in}$ / $E_{total,in}$

C-neutral CO generation 2.25 mol/MJ
7/4 mol CO / (η_{total} x $E_{total,in}$)

fossil CO_2 generation 0.89 mol/MJ
0.69 mol CO_2 / (η_{total} x $E_{total,in}$)

Figure 3. To assess process viability (compare to Figure 2).

(A) Assumed as a completely reversible process, (B) as lower heating value of coal converted at 35% efficiency to electricity, and (C) the synthesis loop (label 10) is computed as succession of isochoric operations recovering a total of > 99.5 mol % of the NH_3 formed.

Bosch-based approaches to solar thermochemical NH_3 synthesis appear potentially economically competitive.

The nitride-based process has three products (NH_3, CO, and electricity) vs. two products with the reforming-based process (NH_3 and CO). This couples both processes to the economics of different products and markets. CO may be used for the production of methanol or Fischer-Tropsch chemicals. The dependency on the inherent byproduction of these chemicals can be lowered via reactant optimization for the nitride-based process (e.g., aiming at a decreased ratio of d/b in Eqs. 1–3 or use of alternative reducing agents such as H_2 if the Gibbs free energy of formation of the metal oxide is sufficiently low) or employment/development of alternative technologies for N_2 separation from air for the reforming-based process. The amount of cogenerated electricity in the nitride-based process can be addressed by optimization of the reactive material as well (see previous paragraph).

No fossil resources are consumed with the nitride-based process which thereby avoids inherently the emission of fossil CO_2. The mechanical energy required for the reforming-based process (for compressing the synthesis gas to 30 MPa, label 8, and for the synthesis loop, label 10, Figure 3) leads to fossil CO_2 emissions when generating electricity from the current energy mix (see "Introduction"). Avoidance of these emissions would require the on-site generation of electricity from renewable resources in the future.

Another factor favoring the nitride-based process, 63% of the total energy input to the nitride-process is absorbed solar heat (absorption losses due to re-radiation not accounted for). The reforming-based process integrates only 19% solar heat. This factor can be increased to 44% if all electricity consumed would be generated (at an efficiency of 30%, see before) from solar heat.

These various facets demonstrate that the assessment of the economic competitiveness depends highly on the current economy (e.g., presence or absence of CO_2 emission regulations, cost of heliostats for concentrating solar energy, etc.). An economic analysis (e.g., a net present value analysis) exceeds the scope of this work and will be presented elsewhere. Concerning the nitride-based process, the sensitivity of process efficiency to the reactant choice offers the possibility to optimize via reactant composition as shown later.

Desirable material properties of the reactant

Major criteria for selecting a reactant constituent (M in Eqs. 1–3) are:

1. moderate to high-nitridation yields of the metal with acceptable kinetics,
2. moderate to high yield of NH_3 from the metal nitride with acceptable kinetics,
3. metal oxide reduction temperature which can be contained in an industrial-scale, solar-heated reactor,[12,29] and that is near the optimal temperature of the reactor receiving solar radiation,[11] see section "Gibbs free energy mapping of chemical elements,"
4. reactant regeneration using a sustainable reducing agent (preferably a gas[30]) in economically attractive quantities,[12,25] see section "Process viability,"
5. absence of melting and boiling of the reactant to avoid pipe blocking, decreased reactant porosity, or cumbersome gas phase separations[31,32] (for possible benefits of gaseous reaction *products*, see section "Step two: Formation of Mg_3N_2"),
6. low to moderate amount of heat liberated by exothermic reactions at temperatures significantly below the temperature of the metal oxide reduction (which absorbs this heat as solar radiation at high-temperatures dependent on the metal oxide stability), see section "Process viability,"
7. acceptable cost and availability of the reactive material[10] and absence of toxicity to humans or the environment[30] (in particular when biomass is used as reducing agent leading to the need for ash disposal, see Figure 1),
8. low number of chemical reactions to reduce complexity,[30]
9. low number of separation steps due to an otherwise increased energy demand[30] (except for gas-liquid or gas–solid separations, see Figures 2 and 3),
10. high ratio of solar energy used as process energy.

Theory and Modeling

A rationale to guide the reactant choice for nitride-based solar thermochemical NH_3 synthesis is proposed here. The simplified theoretical approach is based on the analysis of the Gibbs free energy of Eqs. 1–3 for various elements and the computation of chemical equilibrium compositions.

Gibbs free energy analysis

Molar Gibbs free energy of formation data (g_f) for various nitride/oxide pairs in the literature,[23,33] and used previously for similar computations,[32] were used here to perform a thermodynamic analysis computing the Gibbs free energy of reaction ($\Delta_{rxn}G$)

$$\Delta_{rxn}G = \sum_{i=\text{products}} n_i g_{f,i} - \sum_{j=\text{reactants}} n_j g_{f,j} \tag{4}$$

where n are the mols of reactants j or products i, and $\Delta_{rxn}G$ in kJ/mol is negative if the reaction is thermodynamically favored at equilibrium in a closed system, i.e., the reaction yield exceeds a half-stoichiometric conversion of reactants. The behavior in an open (flow-through) system may differ substantially from thermodynamic predictions due to nonequilibrium situations including mass transfer. However, thermodynamics is used here as a starting point. The absolute error of g_f was estimated previously with $\pm$ 3 kJ[32] and was taken as 2% of the value in kJ/mol. Error propagation was used to estimate the error of $\Delta_{rxn}G$ values computed.

Computation of equilibrium compositions

Assuming ideal gases and ideal condensed phase's yields[34]

$$K_T = \exp\left[-\frac{\Delta_{rxn}G}{RT}\right] = \prod_{i=\text{products}} n_i^{si} \prod_{i=\text{reactants}} n_i^{-sj} \left(\frac{p}{n}\right)^{si-sj} \tag{5}$$

where K_T is the dimensionless equilibrium constant of a given reaction as a function of temperature (T) in K. R is the gas constant in kJ/mol/K, S_i and S_j are reaction stoichiometric coefficients, p is the total pressure in MPa, and n in mol is the total number of chemical species in the system, for simplicity taken as the arithmetic mean of the number of reactants and the number of products at complete conversion. Equations 4 and 5 together with the elemental mol balances of a given reaction system were solved numerically (MathCad 13) to yield the equilibrium composition as a function of T at 0.1 MPa (e.g., $MgO_{(s)} + C_{(s)} \leftrightarrow Mg_{(g)} + CO_{(g)}$ yielding $n_{CO} = (K_T^{1/2} - K_T)/(1 - K_T)$, carbide formation disregarded). It is indicated below when $\Delta_{rxn}G$ calculations were extrapolated using a linear fit

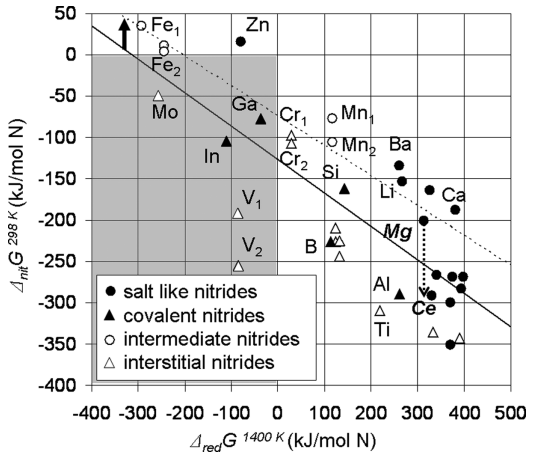

Figure 4. Utility of various elements for reactive NH_3 synthesis at atmospheric pressure: $\Delta_{rxn}G$ of metal nitridation (Eq. 2) vs. $\Delta_{rxn}G$ of carbothermal metal oxide reduction (Eq. 1).[23,33]

Selected nitride/oxide pairs (see "Thermochemical trends of metal nitride/oxide formation") are represented with the chemical symbol of the metallic constituent (subscript "2" marks lower nitrides, e.g., Fe_4N/Fe_2O_3 marked with Fe_2, Fe_2N/Fe_2O_3, marked with Fe_1). A complete description of the diagram is provided in additional online materials. The tradeoff region of negative $\Delta_{rxn}G$ for nitride formation *and* oxide reduction is the gray rectangular area. A linear fit is marked with a solid line. The computation is repeated for nitridation at 1,000 K (or lower, limited by available data), represented by a linear fit (dashed line, no individual data points shown).

(R^2 generally $>$ 0.999) (see other chemical equilibrium software such as STANJAN). Generally, g_f values were extrapolated for $Mg_3N_{2(s)} > 1{,}300$ K, for $Mg_{(g)} > 2{,}000$ K and for N_2 and CO $> 2{,}500$ K.

Thermochemical Trends of Metal Nitride/Oxide Formation

The following provides a thermodynamic analysis of 35 candidate nitride/oxide pairs (Li_3N/Li_2O, Be_3N_2/BeO, BN/B_2O_3, Mg_3N_2/MgO, AlN/Al_2O_3, Si_3N_4/SiO_2, Ca_3N_2/CaO, ScN/Sc_2O_3, TiN/TiO_2, VN/V_2O_5, $VN_{0.465}/V_2O_5$, CrN/Cr_2O_3, Cr_2N/Cr_2O_3, Mn_5N_2/MnO, Mn_4N/MnO, Fe_2N/Fe_2O_3, Fe_4N/Fe_2O_3, Co_3N/Co_3O_4, Zn_3N_2/ZnO, GaN/Ga_2O_3, Sr_3N_2/SrO, YN/Y_2O_3, ZrN/ZrO_2, NbN/Nb_2O_5, Nb_2N/Nb_2O_5, Mo_2N/MoO_2, InN/In_2O_3, Ba_3N_2/BaO, CeN/CeO_2, HfN/HfO_2, TaN/Ta_2O_5, Ta_2N/Ta_2O_5, Th_3N_4/ThO_2, ThN/ThO_2, and UN/UO_2) to guide the material selection for the reactive NH_3 synthesis. Focusing on a single element of this selection will furthermore require consideration of boiling points (see, e.g., Mg in the section "Promising elements for the nitride formation, and NH_3 liberation step"), kinetics (see section "Tradeoff elements") and different oxidation states of the metal (see, e.g., Mn(IV) to Mn(II) in the section "Step two: Formation of Mg_3N_2").

The analysis quantifies a correlation between thermodynamically favorable metal nitridation and NH_3 liberation via hydrolysis and undesirable strong metal-oxide bonds formed during hydrolysis. Nitride-based NH_3 synthesis may be realized with elements representing a tradeoff (the gray region in Figures 4 and 5) of these conflictive, thermochemical properties. However, these elements may cause only moderate NH_3 yields above 298 K (e.g., Mo,[35] Figure 5) or require activation of the N_2 before fixation (e.g., Zn,[36] Figure 4, see section "Promising elements for the NH_3 liberation and oxide reduction step").

An alternative approach, combining elements far outside this tradeoff region to manufacture a mixed material incorporating two desired reactive properties is conceivable. This will be explored selecting Mg or Ce for their high-expected yields of fixed nitrogen and liberated NH_3 on the one hand (Figures 4 and 5), and Cr, Mn, Fe or Mo for their tendency to form less stable metal oxides on the other hand (Figure 4).

Gibbs free energy mapping of chemical elements

Figure 4 shows $\Delta_{rxn}G$ of the nitridation reaction ($\Delta_{nit}G$) at 0.1 MPa and 298 K as a function of $\Delta_{rxn}G$ of the carbothermal metal oxide reduction ($\Delta_{red}G$) at 0.1 MPa and 1,400 K (reduction of Co_3O_4 was computed at 1,000 K due to availability of data). The classification of nitrides was taken from the literature.[37] Uncertainties of $\Delta_{rxn}G$ follow a normal distribution with on average $\pm$ 4.01% of $\Delta_{nit}G$ or $\pm$ 20.66% of $\Delta_{red}G$, respectively. Monte Carlo simulation yields the dimensionless slope of a linear regression with -0.40 ± 0.01 (Figure 4).

This trend suggests a necessary tradeoff. The stability of the oxide increases with increasing tendency of a metal to form nitrides. Recovering the metal from stable oxides unfortunately requires high-reduction temperatures aided by carbon as a chemical reducing agent.

Nitridation computed at 1,000 K (except Co_3N at 600 K, Zn_3N_2 at 700 K, and AlN, Ca_3N_2, Cr_2N, CrN, Mn_4N, Mn_5N_2, and Mo_2N at 800 K) is represented by a linear fit (dashed line, individual data points omitted for clarity, for details see Additional Supporting Materials online). Increasing the nitridation temperature to a kinetically reasonable value[37,38] positions some elements that are attractive due to their low metal-oxygen bond energy, at a region with positive $\Delta_{nit}G$, i.e., nitride formation is not favored (Figure 2). Formation of these nitrides requires elevated N_2 pressure and/or nitrogen activation (e.g., plasma dissociation or other

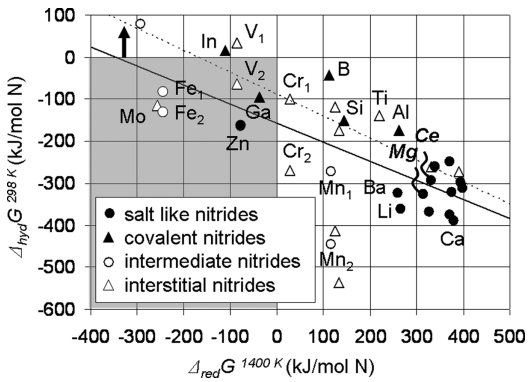

Figure 5. Utility of various elements for reactive NH_3 synthesis at atmospheric pressure: $\Delta_{rxn}G$ of metal nitride hydrolysis (Eq. 3) vs. $\Delta_{rxn}G$ of carbothermal metal oxide reduction (Eq. 1).[23,33]

Selected nitride/oxide pairs are abbreviated such as in Figure 4. A complete description of the diagram is provided in additional online materials. The tradeoff region of negative $\Delta_{rxn}G$ for NH_3 formation *and* oxide reduction is marked (gray rectangle). A linear fit is marked with a solid line. The computation is repeated for corrosion at 800 K (or lower, limited by available data), represented by a linear fit (dashed line, no individual data points shown).

activated N sources)[39] if the nitride is only stable at low temperatures. Low temperatures do not allow useful nitride formation from N_2 due to decreased reaction kinetics.

Plotting $\Delta_{rxn}G$ for hydrolysis ($\Delta_{hyd}G$, ± 19.43% average uncertainty) at 0.1 MPa and 298 K vs. $\Delta_{red}G$ yields the dimensionless slope of a linear regression with -0.45 ± 0.03 (Figure 5). A correlation similar to that in Figure 4 is observed: Elements forming an undesirably strong bond with oxygen tend to liberate NH_3 on nitride hydrolysis. Increasing the hydrolysis temperature[37,38] decreases the tendency for formation of NH_3 and favors undesirable N_2 formation (computed at 800 K, except Co_3N at 600 K, and Zn_3N_2 at 700 K).

Tradeoff elements

Metals that are — at the computed temperatures — elements of both tradeoff regions (Figures 4 and 5), V, Ga, and Mo are only of limited attractiveness for the investigated reaction cycle due to physical material properties and reaction kinetics. Carbothermal reduction of V_2O_5 would require precise temperature control to conduct the initial reduction of V(V) to V(IV) at below 943 K, the melting point of V_2O_5. More importantly, V reduces N_2 only slowly (20–25 h at red glow[20]), and hydrolysis of the vanadium nitrides will results in low NH_3 yields (Figure 5). Nitridation kinetics of Ga and Mo dictate N_2 reduction at above or near the decomposition temperatures of the nitrides (ca. 919 K for GaN or 1115 K for Mo_2N[23]) leading to the need for increased partial N_2 pressures (reportedly 6 MPa for Mo[20] and on the order of GPa for Ga[36,40]).

Promising elements for the nitride formation and NH_3 liberation step

Elements with high $\Delta_{red}G$ (and relatively low $\Delta_{nit}G$ and $\Delta_{hyd}G$) values (Figure 4 and 5) such as the highly electropositive Li, Mg, Ca, Ba and Ce form salt-like nitrides (criteria 1, see "Desirable material properties of the reactant" section). These nitrides are composed mainly of metal cations and N^{3-} anions.[20,37] Hydrolysis of these materials forms NH_3 readily and rapidly[37,38] (criteria 2), but also highly stable oxides (violating criteria 3 and 6).

Regenerating Li_3N from LiOH formed during hydrolysis[20] is further complicated by the low melting point of LiOH at 744 K, which would likely result in undesirable vapor formation of reactants and products at atmospheric pressure during the oxide reduction[23] (violating criteria 5).

MgO is a solid and abundant material (criteria 5 and 7). Due to increased entropy values when forming gases, the reaction equilibrium for carbothermal reduction of MgO favors Mg vapor formation at above about 2,100 K.[23] In an open (nonequilibrium) system carbothermal reduction of MgO at a molar ratio of MgO/C of 1/2 was demonstrated successfully yielding 50 mol % Mg after 30 min at 1,823 K when using wood-derived charcoal as reducing agent.[41] Similar to MgO, reduction of CaO, BaO and CeO_2 forming nitrides requires carbon and relatively high temperatures (Figure 4). Carbothermal reduction of CaO and BaO in the presence of N_2 suppresses the nitride formation completely and has been reported to yield cyanide-like compounds[20] (violating criteria 8). This difficulty to form the nitride directly can be expected for Mg-based reactants as well and is the following focus (see section "Step two: Formation of Mg_3N_2").

The utility of Al for the nitride-based NH_3 synthesis has been demonstrated successfully (see "Introduction").[10,24–26] Intermittent operation and containment of temperatures above 2,000 K required for Al_2O_3 reduction in a large-scale, nonequilibrium reactor will likely require refractory construction materials that constitute a crucial capital cost and construction feasibility factor.[12,20,21] Also, liberation of NH_3 from the highly corrosion-resistant AlN requires high temperatures and, thus, rapid quenching of the NH_3 liberated to prevent decomposition. The utility of Ti can be expected to be comparable to that of Al. The carbothermal reduction of TiO_2 may proceed at slightly lower temperatures than those required for the reduction of Al_2O_3 (Figures 4 and 5). However, hydrolysis of TiN requires high temperatures and appears to yield less NH_3[36] than the hydrolysis of AlN (Figure 5).

Promising elements for the NH_3 liberation and oxide reduction step

Oxides of elements with low $\Delta_{red}G$ (and relatively low $\Delta_{hyd}G$) values, e.g., Fe, Zn and Mo, can be reduced at below 2,200 K without carbon[23] (criteria 4) or at significantly lower temperatures with carbon or H_2 as reducing agent (criteria 3 and 6).

Metals of this group tend not to react with 0.1 MPa N_2 (e.g., Fe[20] and Zn[19,20]) or show low-nitridation yields (e.g., Mo[38]) (violating criteria 1). NH_3 synthesis using Zn_3N_2 has been proposed previously.[42] The high ratio of ionic bonding in Zn_3N_2[37] and the thoroughly studied thermal dissociation of ZnO via solar radiation[11] are attractive. However, N_2 fugacities in equilibrium with Zn_3N_2 and Zn metal are (dependent on temperature) on the order of TPa[36,43] leading to the need for prohibitively high pressurization of N_2 gas when forming Zn_3N_2 from its elements.

Doping a reactant from the first group (e.g., Mg) with an element from this group (e.g., Fe) may aid in decreasing the oxide reduction temperature of a composite material.[31,44–48] Whether this decreases the stability of the ternary nitride[49] relative to the nitride of the first group metal deserves attention when manufacturing a selected material.

Promising elements for the nitride formation and oxide reduction step

Among the remaining elements with intermediate values of $\Delta_{red}G$ (see also section "Tradeoff elements"), B, Si, V, Ga, and In have undesirably low-melting points or form undesirable volatile oxides or hydroxides[23] (violating criteria 5). Perhaps determined by the ionization potential of the metal and the degree of incompleteness of the d-electron orbitals the nitrides of this group are reported to yield only traces of NH_3 upon hydrolysis.[19,20,37,50]

The presence of Cr[50] or Mn in a reactant from the first group might be used to aid the oxide reduction of this element. Whether this affects the ability of the composite reactant to liberate nitrogen in form of NH_3 deserves attention when selecting a dopant from this group.

Mixed Reactants for Thermochemical NH_3 Synthesis

The properties of elemental nitrogen[39] appear to result in a tradeoff in the chemistry of reactive NH_3 synthesis. The high-triple bond energy of the N_2 molecule yields small values of Gibbs free energy for a metal nitride relative to Gibbs free energy values for the corresponding metal oxide.

Table 1. Overview of Thermochemical Concepts to Produce NH_3 from H_2O and N_2 at near Atmospheric Pressure (A) Relative to Mg, and (B) Relative to Fe

Reactant component for N_2 fixation and NH_3 liberation
Mg Advantages
• Mg breaks the N_2 triple bond and forms reactive N^{3-} ions (Mg_3N_2)
• Mg_3N_2 liberates NH_3 quickly via hydrolysis at 0.1 MPa and < 373 K
• abundant, cheap and non-toxic, decreased reactant-makeup costs
Disadvantages, risks and unknowns
• MgO requires carbothermal reduction at ca. 2130 K (closed system)
• Mg_3N_2 decomposes at temperatures required for MgO reduction
• Intermediate Mg metal formation requires rapid product quenching
Ce [A] Advantages
• CeN directly from CeO_2, C, and N_2 at ca. 2150 K (closed system)
Disadvantages, risks and unknowns
• Decreased contribution of ionic bonding in CeN
• Uncertain NH_3 liberation kinetics
• Increased costs for Ce reactant-makeup
Reactant component to aid metal oxide reduction
Fe Advantages
• Increased Mg_3N_2 yield (decreased MgO reduction temperatures)
• abundant, cheap and low toxicity
Disadvantages, risks and unknowns
• Catalyses NH_3 decomposition
• May reduce the concentration of N^{3-} in the reactant
• Increased amount of reducing agent required
Cr, Mn, Mo [B] Advantages
• Contribute to N_2 fixation (Cr, Mn) and NH_3 liberation (Mo)
• Decreased catalytic NH_3 decomposition activity
Disadvantages, risks and unknowns
• Decreased abundance (increased reactant-makeup costs)
• Increased oxide stability (decreased yield of Mg_3N_2) (Cr, Mn)
• Increased oxide volatility (Mo)
Zn [B] Advantages
• Mg/Zn vapor formation may aid two-step nitridation of Mg at decreased temperatures
Disadvantages, risks and unknowns
• Rapid quenching of reaction products required

Therefore, high-metal nitridation yields correlate with formation of highly stable metal oxides formed during hydrolysis of the nitride for NH_3 formation. Analogously, due to the low-electron affinity of nitrogen only the most electropositive elements show a high ratio of ionic bonding[49] correlating with desirable high yields of NH_3 formation and undesirable stable metal-oxygen bonding.

The resulting quandary of obtaining reasonable process conditions with a single chemical element may be resolved by intimately combining two elements with different desired reactant properties in close contact. This has been applied successfully for reactants for solar thermochemical H_2O or CO_2 splitting,[31,44,48] catalysts for NH_3 synthesis,[45,46] and Li-air batteries,[47] and is explored here for Mg-based reactants. From the discussed elements Mg was chosen due to its high potential to reduce N_2 to $2N^{3-}$ and due to the high stability of the formed nitride relative to those formed by Li or Ba for instance (Figure 4). To fix nitrogen in the solid state (in form of a salt-like nitride) at the temperatures required for the oxide reduction step, Ce is proposed as alternative to Mg. Conclusions are summarized in Table 1.

Step one: Reduction of MgM_nO_4 ($M_n = Cr_2, Fe_2, Mo$) reactants

$Mg(OH)_2$ formed during hydrolysis of Mg_3N_2 decomposes at elevated temperatures into highly stable MgO. Reduction of MgO in a closed system requires carbon as reducing agent and technically unsuitable high temperatures of about 2,130 K (Figure 6). Carbothermal reduction of Cr_2O_3 on the other hand is favored thermodynamically at above about 1,500 K (Figure 6). Also, Cr_2O_3 can be reduced with a gaseous reducing agent (criteria 4) and solar radiation.[50] A material such as $MgCr_2O_4$ (i.e., $MgO^*Cr_2O_3$) may be reduced at temperatures significantly below 2,130 K[31,44,48] (Figure 6).

Computations are based on g_f values for oxides of the spinel group. These stable compounds[51] have increased values of g_f[23] relative to the pure metal oxides. Therefore, the presence of a transition metal may allow the reduction of MgO at decreased temperatures due to an increased amount of oxidized reducing agent formed or due to reduction at the solid–solid MgO/transition metal oxide particle boundary. Possible formation of carbides (which tend to convert to oxides during the hydrolysis step) is disregarded at this point. Replacing Cr_2O_3 with Fe_2O_3 or MoO_3 (not shown, see "Thermochemical trends of metal nitride/oxide formation"), respectively, yields $\Delta T_l/\Delta T_h$ values (Figure 6) for the three mixed materials in the range of 0.49–0.98. If such a decrease in the oxide reduction temperature could be realized even partially than the costs for reactor construction materials required to physically contain the reaction temperature could be decreased significantly.

Step two: formation of Mg_3N_2

Mg_3N_2 decomposes (Figure 7B) below the temperature required for carbothermal reduction of MgO (Figure 7A) causing low yields of the nitride when formed directly from the oxide at equilibrium (Figure 8).

This offers the possibility to conduct the NH_3 synthesis cycle in three steps (criteria 1 but violating criteria 8). These are (Figure 2): Carbothermal reduction of $MgO_{(s)}$ forming $Mg_{(g)}$ (Figure 7A), nitridation of a fine $Mg_{(s)}$ powder at decreased temperatures yielding $Mg_3N_{2(s)}$ (Figure 7B), and hydrolysis of $Mg_3N_{2(s)}$ recycling $MgO_{(s)}$ and yielding NH_3 (see "Step three: Hydrolysis of Mg_3N_2 yielding NH_3"). To avoid product recombination during the oxide reduction step this three-step process requires rapid quenching of the Mg/CO vapor.[11,30] A transition metal oxide forming a metal vapor during its reduction (e.g., ZnO) may possibly serve to lower the reduction temperature of the Mg-based reactant (Table 1).

To form the nitride directly from the oxide (criteria 8) one may attempt either to decrease the temperature required for the oxide reduction step or to increase the stability of the nitride at elevated temperature. The first approach (using

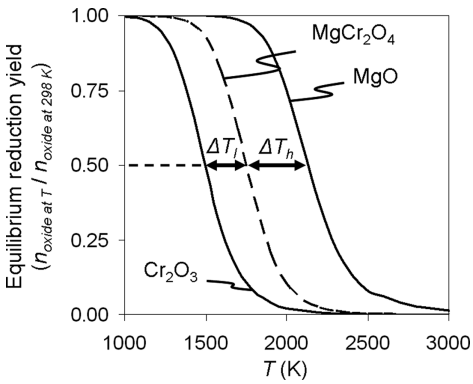

Figure 6. Carbothermal reduction of Cr_2O_3 (extrapolated above 1,800 K), MgO, and $MgCr_2O_4$ (extrapolated above 2,000 K) to the metal.

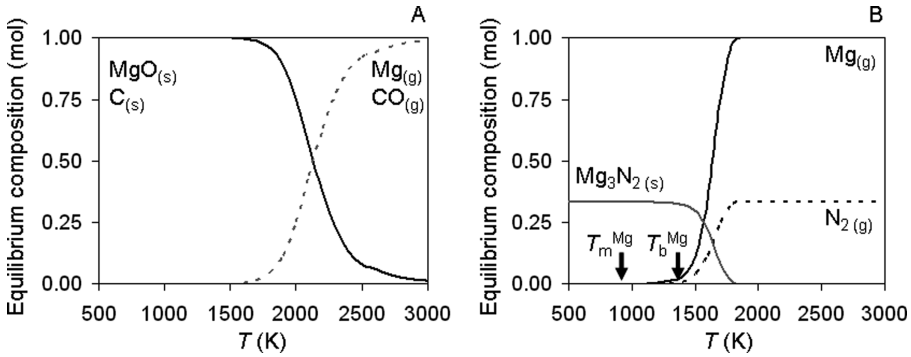

Figure 7. Chemical equilibrium composition of two-step MgO to Mg_3N_2 conversion (endothermic MgO reduction at high temperatures and exothermic nitridation of the condensed metal at decreased temperatures).

Melting (T_m) and boiling (T_b) points of Mg are marked.

reactant doping with transition metals) is demonstrated in the previous section. The theoretical maximum yield of Mg_3N_2 via carbothermal reduction in the presence of N_2, and when introducing various transition metals into the magnesium oxide is shown in Figure 8. Addition of Fe_2O_3 for instance yields at least theoretically at 1,300 K about 64.21 mol % Mg in form of solid Mg_3N_2, 1.02 mol % Mg in form of liquid Mg and the balance solid $MgFe_2O_4$ (see also the additional online materials). Formation of carbides and transition metal nitrides (as expected for Cr and Mo) is for simplicity disregarded. The increased yield of Mg_3N_2 using Fe or Mo as a component for Mg-based reactants has to be weighed against the low vapor pressure of MoO_3[23] (criteria 5), the costs for Mo makeup (criteria 7), and the undesirable catalytic properties of Fe in NH_3 formation and decomposition (criteria 2).

Alternatively, an approach to stabilizing the metal nitride is shown in Figure 4, indicating (dotted arrow) a significant decrease in $\Delta_{nit}G$ by −91.3 kJ/mol N when substituting Mg with Ce. This modification does only slightly increase $\Delta_{red}G$ (+15.9 kJ/mol N) and $\Delta_{hyd}G$ (+32.5 kJ/mol N) (Figures 4 and 5) (criteria 1, 2, and 8). The increased stability of CeN will likely increase the yield of nitrogen in the solid state during the high temperature oxide reduction step circumventing the intermediate formation of a metal phase (Figure 8). The nitride possesses a significant degree of ionic bonding and is expected to liberate sufficient quantities of NH_3 when hydrolyzed.[20]

The temperature required for the direct conversion of CeO_2 to CeN (50 mol % conversion in a closed system at about 2,150 K) might be decreased in a similar way as discussed above for Mg. Due to a limited amount of data for ternary Ce compounds Figure 9 shows an Ellingham diagram of Ce and Mn oxides using carbon or H_2 as reducing agent. The diagram illustrates the possible presence of various oxidation states of Ce and Mn compounds. H_2 may be used to generate lower metallic oxidation states (criteria 4). Metals in lower oxidation states may aid the reduction of metals in higher oxidation states, that is, leading to oxygen transfer from Ce to Mn atoms. However, the reduction of Ce(III) to

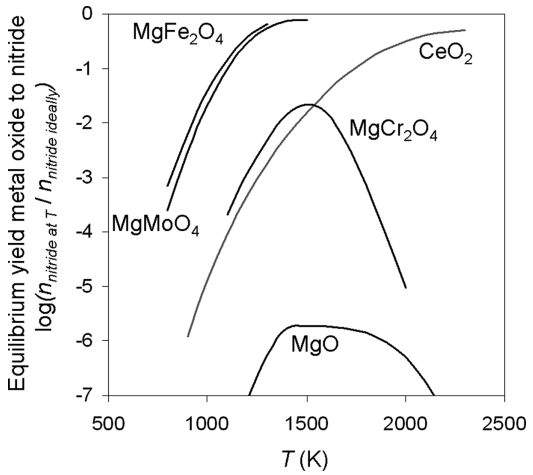

Figure 8. Direct conversion of selected metal oxides to nitrides (i.e., Mg_3N_2 or CeN; the yield of CeN from CeO_2, marked with CeO_2, is extrapolated above 2000 K).

The presence of a transition metal oxide in an alkaline earth metal-based reactant for NH_3 synthesis may allow oxide reduction at decreased temperatures and, thus, increased nitridation yields.

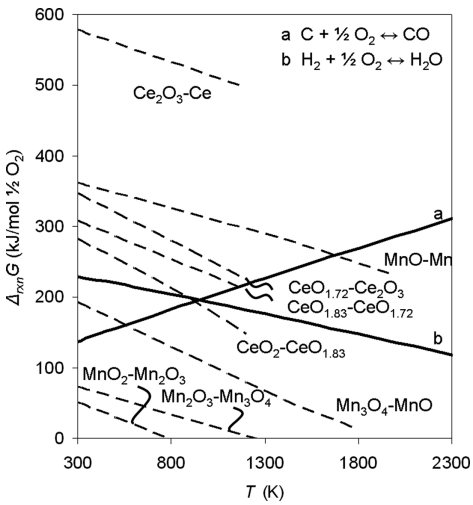

Figure 9. Ellingham diagram for the reduction of oxides of Ce or Mn, respectively.

Removal of 1 atom O from an oxide to form a lower oxidation state (e.g., MnO-Mn abbreviating the equilibrium between MnO and Mn + ½ O_2) occurs spontaneously if its $\Delta_{rxn}G$ reaches 0, or if its $\Delta_{rxn}G \leq \Delta_{rxn}G$ of an oxygen absorbing reaction such as combustion of C or H_2 (a or b).

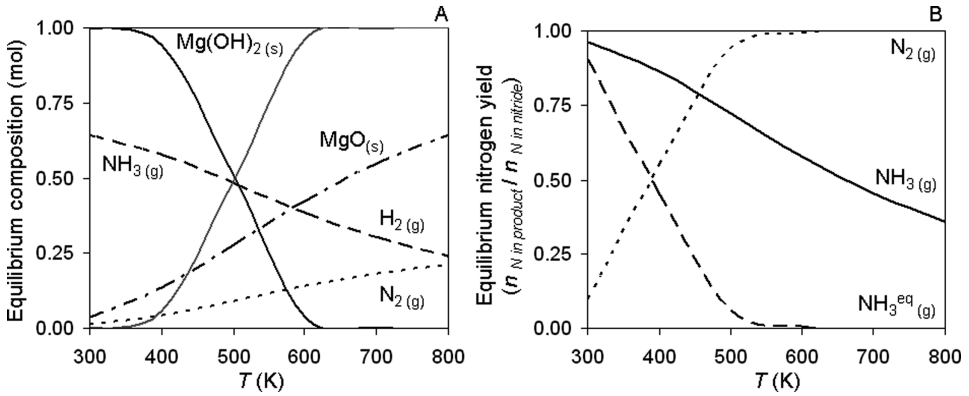

Figure 10. Formation of NH_3 at 0.1 MPa via hydrolysis of Mg_3N_2 ($Mg(OH)_2$ extrapolated above 500 K) (A) and equilibrium yield of N in the gas phase during the hydrolysis if NH_3 is not withdrawn (NH_3^{eq}) from the system and quenched (B).

the metal (Figure 9) or its conversion to CeN (Figure 8) requires high temperatures and a solid, carbonaceous reducing agent such as biomass or charcoal causing ash formation and, thus, the need of some reactant makeup. Technical advantages of Ce for the overall cycle studied here have to be weighed against criteria 4 and 7.

Step three: Hydrolysis of Mg_3N_2 yielding NH_3

To close the cycle, Mg_3N_2 hydrolyzed at 368 K yields NH_3 quickly.[22] Formation of NH_3 at this temperature and at 0.1 MPa total pressures would avoid the need for gas compression since NH_3 is thermodynamically stable at these conditions. The exothermic heat of reaction liberated at near this temperature would be of low value (see criteria 6).

Gibbs free energy analysis shows that hydrolysis of Mg_3N_2 (Fig. 10A) forming $Mg(OH)_2$, N_2 and H_2 is favored at equilibrium over NH_3 formation at above 400–500 K (Fig. 10B). To account for this formation of N_2, the amount of NH_3 liberated from the nitride is estimated here based on the ratio of the equilibrium constants for NH_3 formation relative to N_2 formation decreasing the yield of NH_3 when increasing the hydrolysis temperature (Figure 10A). This illustrates that NH_3 formation via nitride hydrolysis is most promising if nitrides are employed which liberate NH_3 at intermediate temperatures and in a system open to mass exchange (to avoid the decomposition shown in Figure 10B). Maximized NH_3 yields might be promoted by reducing opportunities for surface diffusion of NH_3, and by carefully minimizing any resistance to the mass transfer of NH_3 away from the metal reactant.

The presence of transition metals in the reactant may reduce the ratio of ionic bonding within the nitride and may decrease the yield of NH_3. Bonding in ternary nitrides is, however, not well-understood.[49] Future research quantifying the bonding nature in mixed or ternary nitrides and assessing the catalytic contribution of nitride components to the decomposition of the NH_3 formed[20,45,46] will further the development of a composite reactant for the solar thermochemical NH_3 synthesis near ambient pressure.

Conclusions and Outlook

The thermodynamic equilibrium of the Haber-Bosch reaction — conducted catalytically at 700–900 K — dictates the need for high partial pressures of the reactants, that is, about 22.5 MPa H_2 and 7.5 MPa N_2. Separating the N_2 reduction step from the nitrogen protonation step offers the possibility to conduct both steps at different temperatures, and thereby favorable equilibrium positions at 0.1 MPa. This may avoid the need for sophisticated high-pressure utilities and decrease the reliance on fossil fuels for electricity generation of the conventional NH_3 synthesis.

Using water as source of hydrogen and concentrated solar radiation for process heat leads to a process (Eqs. 1–3) that converts solar energy to chemical energy, stored in NH_3, CO, and electricity. The dependency on the inherent byproduction of electricity may be addressed by control of the reactant composition: The higher the heat of reaction that is absorbed in the endothermic metal oxide reduction step at high temperature (from solar radiation), the higher the heat of reaction of the exothermic NH_3 formation at low temperature (to electric energy byproduct). This thermochemical analysis quantifies furthermore: The higher Gibbs free energy of the metal oxide reduction (need for high reduction temperatures), the lower Gibbs free energy of the NH_3 liberation (high NH_3 yields) (Figure 5).

Given the unfavorable kinetics of the N_2 reduction step of single elements representing a tradeoff of these conflicting properties (V, Ga and Mo) and given the quick formation of NH_3 via hydrolysis of salt-like nitrides (e.g., Li, Mg, Ba and Ce), nitrides with high ionic contribution to the metal-nitrogen bond have been focused here. From this group, Mg and Ce have been selected due to the inferior thermodynamic stability of Li and Ba nitrides (Figure 4), and presumably complicated processing of Li-based reactants (highly volatile oxides and a hydroxide with a low melting point). A qualitative summary of this thermochemical analysis is given in Figure 11.

In principle, MgO may be reduced carbothermally to a metal vapor formed at near 1,800 K in a system open to mass exchange. The condensed metal could, thereafter, be used as electron donor for the N_2 reduction step. However, the conceivable direct conversion of MgO to Mg_3N_2 at decreased temperatures (required due to the decomposition of the nitride at elevated temperatures) is more attractive from a practical perspective since this would greatly simplify processing (rapid quenching to suppress the oxidation of Mg by CO, handling a metal vapor, reactor materials and design for high temperatures). The potential to decrease the

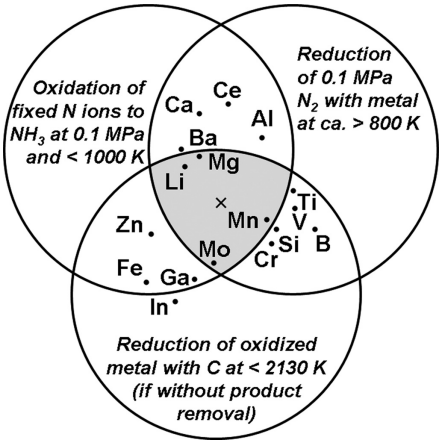

Figure 11. Primary demands of the solar thermochemical NH_3 synthesis on the reactive materials and qualitative summary (see kinetic effects and limited thermochemical data at elevated temperatures above) of the related thermochemical properties for single elements.

The metal oxide reduction temperature was chosen for guidance only. Increasing this temperature or removing reaction products will allow the reduction of all oxides shown. The ideal combination of thermochemical properties is marked with "x".

reduction temperature of the metal oxide by doping with transition metals has been employed for solar thermochemical H_2O or CO_2 cleavage and has been explored here for the Mg-based (i.e., $MgCr_2O_4$, $MgFe_2O_4$, or $MgMoO_4$) solar thermochemical NH_3 synthesis. Future work needs to address experimental verification of this concept (nitride formation near 1,500 K), and of the possibility to increase the nitride stability at higher temperatures by using Ce-based reactants.

Acknowledgments

We thank Dr. Leigh Murray and Dayou Jiang for their assistance with statistical verification. This material is based on work supported by National Science Foundation Grant # 0903701: "Integrating the Socio-economic, Technical, and Agricultural Aspects of Renewable and Sustainable Biorefining Program, awarded to Kansas State University". Funding by the Center for Sustainable Energy, Kansas State University is kindly acknowledged.

Literature Cited

1. Smil V. Population growth and nitrogen: An exploration of a critical existential link. *Population Develop Rev*. 1991;17(4):569–601.
2. Schnepf R, Yacobucci BD. Renewable Fuel Standard (RFS): Overview and Issues. Congressional Research Service; 2010.
3. Kramer DA. Nitrogen (fixed) - Ammonia. *US Geological Survey, Mineral Commodity Summaries*; 2003:118–119.
4. Rafiqul I, Weber C, Lehmann B, Voss A. Energy efficiency improvements in ammonia production - perspectives and uncertainties. *Energy*. 2005;30(13):2487–2504.
5. Ritter SK. The Haber-Bosch reaction: An early chemical impact on sustainability. *Chem Eng News*. 2008;86(33):53.
6. Kirova-Yordanova Z. Exergy analysis of industrial ammonia synthesis. *Energy*. 2004;29(12–15):2373–2384.
7. Thomas G, Parks G. Potential roles of ammonia in a hydrogen economy, a study of issues related to the use ammonia for on-board vehicular hydrogen storage. *US Dept of Energy*; 2006. http://www.hydrogen.energy.gov/pdfs/nh3_paper.pdf (retrieved 12/2011).
8. Christensen CH, Johannessen T, Sørensen RZ, Nørskov JK. Towards an ammonia-mediated hydrogen economy? *Catal Today*. 2006;111(1–2):140–144.
9. Reiter AJ, Kong SC. Combustion and emissions characteristics of compression-ignition engine using dual ammonia-diesel fuel. *Fuel*. 2011;90(1):87–97.
10. Gálvez ME, Halmann M, Steinfeld A. Ammonia production via a two-step Al_2O_3/AlN thermochemical cycle. 1. Thermodynamic, environmental, and economic analyses. *Ind Eng Chem Res*. 2007;46(7):2042–2046.
11. Steinfeld A, Weimer AW. Thermochemical production of fuels with concentrated solar energy. *Optics Express*. 2010;18(9):A100–A111.
12. Kodama T. High-temperature solar chemistry for converting solar heat to chemical fuels. *Progr Energy Combust Sci*. 2003;29(6):567–597.
13. Pool JA, Lobkovsky E, Chirik PJ. Hydrogenation and cleavage of dinitrogen to ammonia with a zirconium complex. *Nature*. 2004;427(6974):527–530.
14. Lerch M, Janek J, Becker KD, Berendts S, Boysen H, Bredow T et al. Oxide nitrides: From oxides to solids with mobile nitrogen ions. *Progr Solid State Chem*. 2009;37(2–3):81–131.
15. Skodra A, Stoukides M. Electrocatalytic synthesis of ammonia from steam and nitrogen at atmospheric pressure. *Solid State Ionics*. 2009;180(23–25):1332–1336.
16. Kongshaug G. Energy consumption and greenhouse gas emissions in fertilizer production. International Fertilizer Industry Association, Technical Conference, Marrakech, Morocco, 28 September-1 October; 1998.
17. http://www.worldcoal.org/resources/coal-statistics/(retrieved 12/2009).
18. Haber F, van Oordt G. Über die Bildung von Ammoniak aus den Elementen. *Z Anorg Chem*. 1905;44:341–378.
19. Lunge G. *Coal-Tar and Ammonia*. London: Gurney and Jackson; 1916.
20. Maxted EB. *Ammonia and the Nitrides*. London, UK: J. & A. Churchill; 1921.
21. Sauchelli V. *Fertilizer Nitrogen its Chemistry and Technology*. New York, NY: Reinhold Publishing Corp; 1964.
22. Glasson DR, Jayaweera SAA. Formation and reactivity of nitrides.2. Calcium and magnesium nitrides and calcium cyanamide. *J Appl Chem USSR*. 1968;18(3):77–83.
23. Barin I, Knacke O. *Thermochemical Properties of Inorganic Substances*. Berlin, Heidelberg, New York: Springer-Verlag; 1973.
24. Gálvez ME, Frei A, Meier F, Steinfeld A. Production of AlN by carbothermal and methanothermal reduction of Al_2O_3 in a N_2 flow using concentrated thermal radiation. *Ind Eng Chem Res*. 2009;48(1):528–533.
25. Gálvez ME, Hischier I, Frei A, Steinfeld A. Ammonia production via a two-step Al_2O_3/AlN thermochemical cycle. 3. Influence of the carbon reducing agent and cyclability. *Ind Eng Chem Res*. 2008;47(7):2231–2237.
26. Gálvez ME, Frei A, Halmann M, Steinfeld A. Ammonia production via a two-step Al_2O_3/AlN thermochemical cycle. 2. Kinetic analysis. *Ind Eng Chem Res*. 2007;46(7):2047–2053.
27. Solar Millennium AG. The parabolic trough power plants Andasol 1 to 3. http://www.solarmillennium.de/upload/Download/Technologie/eng/Andasol1–3engl.pdf (retrieved 11/2011).
28. Ramezan M, Skone TJ, ya Nsakala N, Liljedahl GN. Carbon dioxide capture from existing coal-fired power plants. National Energy Technology Laboratory, final report (original issue date, December 2006) 2007;DOE/NETL-401/110907.
29. Murray JP, Steinfeld A, Fletcher EA. Metals, nitrides, and carbides via solar carbothermal reduction of metal-oxides. *Energy*. 1995;20(7):695–704.
30. Perret R. Solar thermochemical hydrogen production research (STCH), Thermochemical cycle selection and investment priority. Sandia report SAND2011–3622, Sandia National Laboratories; 2011.
31. Miller JE, Allendorf MD, Diver RB, Evans LR, Siegel NP, Stuecker JN. Metal oxide composites and structures for ultra-high temperature solar thermochemical cycles. *J Mater Sci*. 2008;43(14):4714–4728.
32. Lundberg M. Model-calculations on some feasible 2-step water splitting processes. *Int J Hydrogen Energy*. 1993;18(5):369–376.
33. Barin I, Knacke O, Kubaschewski O. *Thermochemical Properties of Inorganic Substances*. Berlin, Heidelberg, New York: Springer-Verlag; 1977 (suppl).
34. Scott Fogler H. *Elements of Chemical Reaction Engineering*. Upper Saddle River, NJ: Prentice Hall PTR; 2006.
35. Samsonov GV. *Handbook of the Physicochemical Properties of the Elements*. London, UK: Oldbourne Book Co; 1968.
36. Juza R. Über die Nitride der Metalle der ersten großen Periode. *Angewandte Chemie*. 1945;58:25–30.
37. Pierson HO. *Handbook of Refractory Carbides and Nitrides*. Westwood, NJ: Noyes Publications; 1996.

38. Glasson DR, Jayaweer SAA. Formation and reactivity of nitrides.I. Review and introduction. *J Appl Chem USSR*. 1968;18(3):65–77.
39. DiSalvo FJ. *New ternary nitrides*. In: *Nitrides and Oxynitrides, Proceedings of the Second International Symposium on Nitrides*, Limerick, Ireland. 2000;325–326:3–9.
40. Yamada T, Yamane H, Ohta T, Goto T, Yao T. Preparation of GaN crystals by heating a Li_3N-added Ga melt in Na vapor and their photoluminescence. *Crystal Res Technol*. 2007;42(1):13–17.
41. Gálvez ME, Frei A, Albisetti G, Lunardi G, Steinfeld A. Solar hydrogen production via a two-step thermochemical process based on MgO/Mg redox reactions - Thermodynamic and kinetic analyses. *Int J Hydrogen Energy*. 2008;33(12):2880–2890.
42. Kaiser K. Verf. zur gewinnung von zinknitrid und ammoniak. *Z Angew Chem*. 1914;27(2):481.
43. Wriedt HA. The N-Zn (nitrogen-zinc) system. *Bull Alloy Phase Diag*. 1988;9(3):247–251.
44. Roeb M, Müller-Steinhagen H. Concentrating on solar electricity and fuels. *Science*. 2010;329(5993):773–774.
45. Jacobsen CJH. Novel class of ammonia synthesis catalysts. *Chem Commun*. 2000(12):1057–1058.
46. Jacobsen CJH, Dahl S, Clausen BS, Bahn S, Logadottir A, Nørskov JK. Catalyst design by interpolation in the periodic table: Bimetallic ammonia synthesis catalysts. *J Am Chem Soc*. 2001;123(34):8404–8405.
47. Jacoby M. Rechargeable metal-air batteries. *Chem Eng News*. 2010;88(47):29–31.
48. Scheffe JR, Li JH, Weimer AW. A spinel ferrite/hercynite water-splitting redox cycle. *Int J Hydrogen Energy*. 2010;35(8):3333–3340.
49. Gregory DH. Structural families in nitride chemistry. *J Chem Soc Dalton Trans*. 1999(3):259–270.
50. Michalsky R, Pfromm PH. Chromium as reactant for solar thermochemical synthesis of ammonia from steam, nitrogen, and biomass at atmospheric pressure. *Solar Energy*. 2011;85(11):2642–2654.
51. El-Shobaky GA, Mostafa AA. Solid-solid interactions in Fe_2O_3/MgO system doped with aluminum and zinc oxides. *Thermochim Acta*. 2003;408(1–2):75–84.

Manuscript received Jun. 30, 2011, and revision received Dec. 3, 2011.